Journal of Materials Chemistry B

Accepted Manuscript

ROYAL SOCIETY OF CHEMISTRY

www.rsc.org/materialsB

Journal Name

Cite this: DOI: 10.1039/c0xx00000x

www.rsc.org/xxxxxx

ARTICLE TYPE

Noncovalent functionalization of mesoporous silica nanoparticles with amphiphilic peptides

Melis Sardan,[‡a,b] Adem Yildirim,[*‡a,b] Didem Mumcuoglu,[a,b] Ayse B. Tekinay, [*a,b] and Mustafa O. Guler[*a,b]

Received (in XXX, XXX) Xth XXXXXXXXX 20XX, Accepted Xth XXXXXXXXX 20XX
DOI: 10.1039/b000000x

The surface of mesoporous silica nanoparticles (MSNs) have been modified for enhancing their cellular uptake, cell targeting, bioimaging, and controlled drug release. For this purpose, covalent anchorage on silica surface was predominantly exploited with a wide range of bioactive molecules. Here, we describe a facile self-assembly method to prepare a hybrid peptide silica system composed of octyl-modified mesoporous silica nanoparticles (MSNs) and peptide amphiphiles (PAs). Hydrophobic organosilane surface of mesoporous silica was coated with amphiphilic peptide molecules. The peptide functionalized particles exhibited good cyto-compatibility with vascular smooth muscle and vascular endothelial cells. The peptide coating also improved the cellular uptake of particles up to 6.3 fold, which is promising for development of highly efficient MSN based theranostics agents.

Introduction

Mesoporous silica nanoparticles (MSNs) have high specific surface area, large pore volume, controlled particle size and morphology, and low inherent toxicity. They are promising platforms for theranostics applications.[1-3] Previously, *in vitro* studies with MSNs demonstrated that these materials can be used as drug delivery and cell marking agents.[4-6] However, it was observed that bare silica surface (contains reactive silanol groups) can cause aggregation of particles and opsonization in biological environment, and nonspecifically interact with the membrane of several cell types, which results in poor biocompatibility and pharmacokinetics for *in vivo* applications.[7-11] Modification of the reactive MSN surface with polymers[12-15] (e.g. PEG and zwitterionic copolymers), small molecules[10, 16] (e.g. phosphonate) or biomolecules[17-19] (e.g. antibodies, peptides, lipid bilayers, DNA and aptamers) has been proved to be an effective way to improve the biocompatibility of particles as well as the efficiency of MSN based therapies. In particular, short peptide chains have attracted a great deal of attention in recent years because of their tunable functionality, biodegradability, and relatively ease of synthesis.[20-22] It has been shown that short peptide sequences (e.g. RGD and IL-13) can be used for targeting nanoparticles to specific cancer cell lines.[22-26] In addition to targeting property, some peptide sequences (e.g. TAT peptide) demonstrated cell penetrating and endosomal escape properties.[27-29] Also, biodegradability of peptides makes them suitable for being utilized as stimuli responsive gatekeepers in controlled drug release[30-31] and linkers in FRET based diagnostics.[32-34]

Conventionally, peptides are covalently attached to the silica surface by using additional cross-linking reagents and troublesome synthetic methods, which result in poor surface grafting density and costly synthesis of functionalized materials.[24, 30, 35] In this work, we demonstrate a simple and cost-effective self-assembly approach to prepare peptide functionalized MSNs, as a promising alternative for covalent attachment methods.[13] Our method is based on the spontaneous attachment of peptide amphiphiles (PAs) to the octyl modified MSN surfaces in aqueous media through hydrophobic interactions between octyl groups of MSNs and alkyl chains of PAs (Scheme 1a). We selected two model PA molecules, with different charges, to functionalize MSNs. The glutamic acid and lysine residues on the PAs provide negative and positive charges to the hybrid system, respectively (Scheme 1b). The unmodified MSN was synthesized in order to compare with peptide functionalized MSNs. The effect of peptide functionalization on cell viability and uptake was investigated by using human umbilical vein endothelial cells (HUVEC) and a vascular smooth muscle cell line (A10). All of the MSN systems demonstrated good cyto-compatibility with both cell lines up to a concentration of 200 μg mL^{-1}. Interestingly, we observed a remarkable increase (1.8 to 6.3 fold) in the cellular uptake of peptide functionalized MSNs compared to bare MSNs depending on the surface charge of PAs and as well as the cell type.

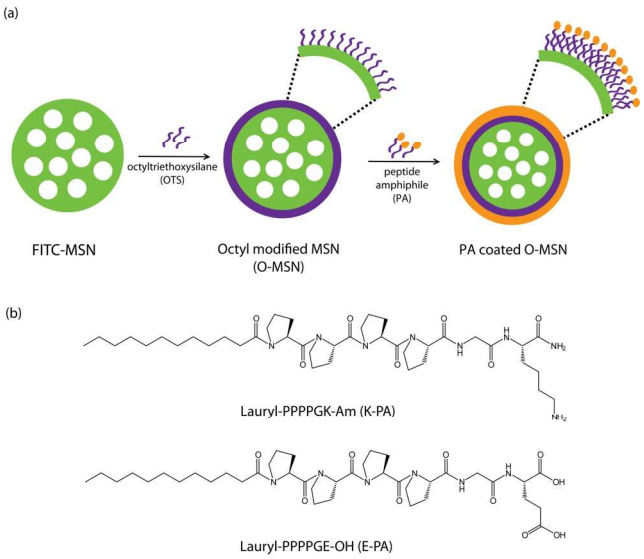

Scheme 1 (a) Schematic presentation of preparation of peptide functionalized MSNs. (b) Chemical structures of the peptide amphiphile molecules used in this study.

Experimental Section

Materials

9-Fluorenylmethoxycarbonyl (Fmoc) and *tert*-butoxycarbonyl (Boc) protected L-amino acids, [4-[α-(2',4'-dimethoxyphenyl) Fmocaminomethyl]phenoxy]acetamidonorleucyl -MBHA resin (Rink amide MBHA resin), and 2-(1*H*-Benzotriazol-1-yl)-1,1,3,3 tetramethyluronium hexafluorophosphate (HBTU) were purchased from NovaBiochem and ABCR. Tetraetyl orthosilicate (TEOS), octyltriethoxysilane (OTS), aminopropyl triethoxysilane (APTES), sodium hydroxide, lauric acid were purchased from Merck. Fluorescein isothiocyanate (FITC), and cetyltriammoniumbromide (CTAB) ethanol were purchased from Sigma-Aldrich. Methanol was purchased from Carlo-Erba. Tetrahydrofuran (THF) was purchased from Labkim. All reagents and solvents were used as provided. Cell culture chemicals were purchased from Gibco, Life Technologies.

Synthesis of MSN and OMSN

In order to synthesize FITC labelled OMSNs, 2 mg of FITC was conjugated to 10 µL of APTES in 1 mL of ethanol by gently stirring for 24 h. Then, 200 mg of CTAB and 6 mg of F127 were dissolved in 96 mL of deionized water and 0.7 mL of 2 M NaOH was added. The solution was heated to 80 °C under vigorous stirring (600 rpm). After the temperature of the reaction mixture was stabilized at 80 °C, 1 mL of TEOS and FITC solution were rapidly added. After 75 min, 0.2 mL of OTS was dissolved in 10 mL THF and slowly added to the reaction mixture in order to form octyl-containing shell. The mixture was further stirred for 90 min. Finally, particles were collected by centrifugation at 9000 rpm and washed with methanol twice. Surfactant extraction was performed by stirring the particles in 50 mL of 20 g L^{-1} ethanolic ammonium nitrate at 60 °C for 1 h. This treatment was repeated twice to ensure complete surfactant removal. Particles were washed with ethanol twice and dried at 50 °C overnight. MSN was synthesized by using the same parameters with the exception of OTS addition.

Synthesis and Characterization of Peptide Amphiphile Molecules

The positively charged peptide amphiphile (K-PA) was constructed on MHBA Rink Amide (0.59 mmol/g loading) resin, and negatively charged peptide amphiphile (E-PA) was constructed on Fmoc-Glu-Wang (0.64 mmol/g loading) resin. All amino acid couplings were performed with 2 equivalents of Fmoc protected amino acid, 1.95 equivalents of HBTU and 3 equivalents of N,N-diisopropylethylamine (DIEA) in DMF for 2 h. Fmoc removals were performed with 20% piperidine/dimethylformamide (DMF) solution for 20 min. Cleavage of the peptides from the resin was carried out with a mixture of trifluoroacetic acid (TFA) : triisoproplysilane (TIS) : water in the ratio of 95 : 2.5 : 2.5 for 2 h. Excess TFA was removed by rotary evaporation. The remaining viscous peptide solution was treated with ice-cold diethyl ether and the resulting white pellet was freeze-dried. The peptide amphiphiles were identified and analyzed by reverse phase HPLC on an Agilent 6530 accurate-Mass Q-TOF LC/MS equipped with an Agilent 1200 HPLC. An phenomenex Luna 3µ C8 100A (50 x 3.00 mm) column as stationary phase and water/acetonitrile gradient with 0.1% volume of formic acid as mobile phase were used to identify positively charged peptide amphiphile. For negatively charged peptide amphiphile, an Agilent Zorbax Extend-C18 (2.1 x 50 mm) column as stationary phase and water/acetonitrile gradient with 0.1% volume of ammonium hydroxide as mobile phase were used. The positively and negatively charged peptide amphiphiles were purified by using 1200 Agilent HPLC on Zorbax 300SB C8 (21.2 x 150 mm) PrepHT and Zorbax-Extend C18 (21.2 x 150 mm) PrepHT column, respectively.

Coating the OMSN with Peptide Amphiphiles

While 14 mg of each peptide amphiphile was sonicated in 12 mL deionized water, 2 mg of OMSN was slowly added to the system. Peptide amphiphiles and OMSN were mixed with a weight ratio of 1:7. They were sonicated and vortexed for 3 h at room temperature. Solution was centrifuged at 5000 rpm. After all portions were concentrated by centrifugation, they were rinsed with water and centrifuged twice.

Characterization of the Particles

Hydrodynamic size and zeta potential of the particles were measured by zetasizer. A Malvern Nanosizer/Zetasizer nano-ZS ZEN 3600 (Malvern Instruments, USA) instrument was used for the analysis. Measurements were performed in glass cuvettes and repeated at least three times. TEM images were obtained with FEI Tecnai G2 F30 TEM at 300 kV. Samples for imaging were prepared by diluting PA coated MSNs to 0.01% (w/v) on a 200-mesh cupper TEM grid for 5 min without staining and air dried. Fluorescence spectra of the particles were recorded by a Varian Eclipse spectrophotometer with an excitation wavelength of 488 nm. FTIR spectra of particles and PAs were collected by using a FTIR (Vertex 70, Bruker). Thermal gravimetric analyses (TGA) were performed with Q500 (TA Instruments). The temperature was increased from room temperature to 800 °C with a rate of 20 °C min^{-1} under nitrogen gas.

Cell Culture Experiments

Viability and uptake experiments were performed by using human umbilical vein endothelial cells (HUVECs) and A10 rat aortic smooth muscle cells (ATCC® Cat# CRL-1476™). HUVECs were donated by Yeditepe University, Istanbul, Turkey. HUVECs were purified as described[36] and characterized by staining with CD34, CD31, and CD90 surface markers. These cells were found to be positive for CD31 and CD34 but negative for CD90. A10 and HUVEC cells were cultured in 75 cm^2 polystyrene cell culture flasks with standard medium, containing Dulbecco's modified eagle medium (DMEM) with 10% fetal bovine serum (FBS), and 1% penicillin/streptomycin and passaged at cell confluency between 80 to 90% using trypsin/EDTA. In all experiments, particles were administered in serum free medium (1% penicillin/streptomycin containing DMEM) to avoid any influence of serum proteins on uptake mechanism.

Cell Viability Tests

Cell viability assay was performed with Alamar Blue Assay (Invitrogen). 5000 cells/well (HUVEC or A10) were seeded on 96 well plate in 100 µL of standard medium. After 24 h, medium was removed and 100 µL of serum free medium was added. 25 µL of freshly prepared nanoparticle solutions in water at different concentrations were administered to have a final concentration of 200, 100, 50, and 10 µg mL^{-1}. For cell viability tests, cells were exposed to particles for 4 h then medium was changed to standard medium and cells were further incubated for 20 h. Then, Alamar Blue reagent diluted to 10% in DMEM was added. After 3 h, fluorescence at 570/612 nm (Ex/Em) was measured with a microplate reader (SpectraMax, M5).

Cellular Uptake Analyses

13 mm glass coverslips were placed in 24 well plates, and 4 x 10^4 cells (HUVEC or A10) in standard medium were seeded in each well. After 24 h, medium was discarded, and 400 µL of serum free medium was added to each well. 100 µL of bare or functionalized MSN particles were administered to have a 200 µg mL^{-1} final concentration of MSN. After 4 h, medium was exchanged to standard medium. After 20 h, cells were washed with PBS several times and fixed with 4% paraformaldehyde for 15 min. Then, cells were permeabilized with 0.1% TritonX-100 (Sigma-Aldrich) for 12 min and actin proteins were stained with Phalloidin-TRITC (Sigma-Aldrich) for 20 min. Coverslips were mounted on slides with Antifade (Invitrogen). Samples were visualized under laser scanning confocal microscopy (Zeiss, LSM 510).

Flow Cytometer Analysis

1 x 10^5 HUVEC or A10 cells/well were seeded in 6 well plates in standard medium. Medium was discarded after 24 h, and 1600 µL of serum free medium was added in each well. 400 µL of bare or functionalized MSN particles were administered to have a 200 µg mL^{-1} final concentration of MSN. After 4 h, medium was changed to standard medium and cells were incubated for 20 h, then washed with PBS and trypsinized. Cells were collected by centrifugation, and washed twice with PBS, and resuspended in 1 mL PBS and kept on ice before analysis. FITC channel was used to analyze MSN particle uptake in flow cytometer (BD, FACS Aria III). Non-treated cells were used as control. Student's t-test was applied to all datasets and a p value of less than 0.05 was accepted to be statistically significant.

Results and Discussion

Synthesis and characterization of peptide functionalized MSNs

Octyl modified water insoluble MSNs (OMSN) were synthesized according to our previous reports[13, 37] by using a one-pot respective condensation method.[38] Tetraethyl orthosilicate (TEOS) molecules were condensed in basic conditions and initial MSNs were formed. Then, octyl triethoxysilane (OTS) molecules were added to the reaction mixture to coat the MSNs with a hydrophobic octyl layer. The fluorescein isothiocyanate (FITC) molecules were conjugated to the MSNs in first step of the synthesis to track the uptake of particles by using confocal imaging and flow cytometer methods.[16] Successful conjugation of FITC to silica network was demonstrated by using fluorescence spectroscopy, where emission bands of FITC molecules were clearly observed (ESI†, Fig. S1). Bare MSNs were prepared for control experiments under the same experimental conditions without the OTS addition. Peptide amphiphiles were synthesized by solid phase peptide synthesis method based on orthogonal protection and verified by liquid chromatography and mass spectrometry (ESI†, Fig. S2 and S3).

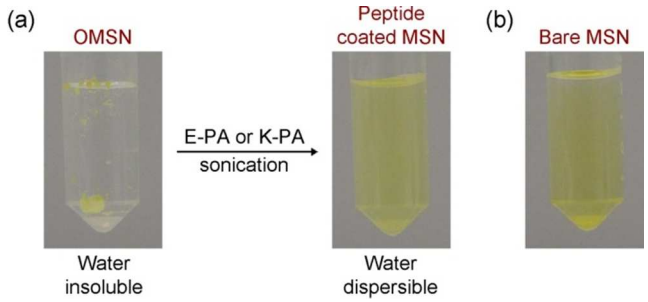

Fig. 1 (a) Photographs showing the water dispersion of OMSNs before and after coating with peptide amphiphiles and (b) Photograph of MSN dispersion in water.

OMSNs were coated with peptide amphiphile molecules by simple sonication in E-PA or K-PA solutions (Fig. 1a). As-prepared OMSNs are insoluble in water (Fig. 1a left) because their surface is covered with hydrophobic octyl groups. After the addition of PA solution and ultrasonication, PA molecules self-assemble on the OMSNs due to hydrophobic interactions between alkyl chains of both OMSN and PA (Scheme 1a). Functionalization with peptide amphiphiles renders the MSNs water dispersible by providing either positively or negatively charged water soluble moieties on their surfaces. Photograph of MSNs dispersed in water is shown in Fig. 1b. Both dispersions have light green color due to the covalently conjugated FITC molecules. Fig. 2 shows the TEM images of the particles. Bare MSNs exhibited MCM-41 type highly ordered hexagonal porous structure (Fig. 2a). On the other hand, for OMSNs, a randomly porous thin shell was observed over a MCM-41 type porous core

(Fig. 2b) which is in accordance with our previous work.[13] After coating the OMSNs with E-PA a thin organic layer was observed around the particles (Fig. 2c). In addition, TEM image of K-PA peptide coated OMSNs is provided in the ESI† (Fig. S4).

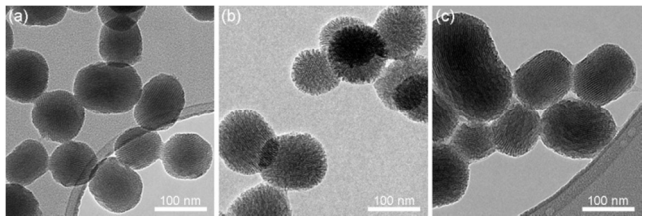

Fig. 2 Characterization of the mesoporous silica nanoparticles. TEM images of (a) MSN, (b) OMSN and (c) E-OMSN.

Formation of peptide coating over OMSNs was further proved by using FTIR and TGA methods. Fig. 3a shows the FTIR spectra of the particles. The –CH peaks between 2800 cm^{-1} and 3000 cm^{-1} were observed in the spectrum of OMSN indicating the successful octyl modification. These absorption bands became stronger for PA modified particles (E-OMSN and K-OMSN) due

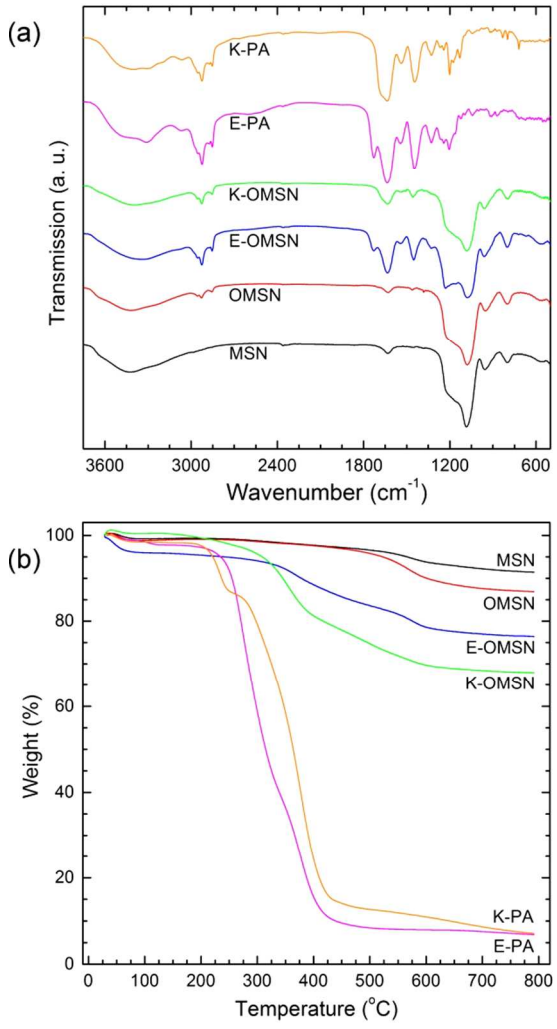

Fig. 3 FTIR spectra (a) and TGA spectra (b) of particles and peptide amphiphiles.

to the –CH bonds of the PAs. In addition, new absorption bands between 1400 cm^{-1} and 1800 cm^{-1} appeared, which are in good agreement with FTIR spectra of the PAs. In addition, Amide I (1600−1690 cm^{-1}, C=O stretching) and amide II (1480−1575 cm^{-1}, CN stretching, NH bending) bands of PAs were observed for PA functionalized MSNs. Another C=O stretching vibration was also observed for glutamic acid containing particles at around 1725 cm^{-1} which corresponds to the side chain of the glutamic acid.

Fig. 3b shows the TGA analysis of the particles. For MSNs, a small weight loss of 7.8% was observed between 100 °C and 800 °C due to the dehydroxylation of the silica surface.[39] The weight loss increased to 11.9% for OMSNs and most of the weight loss occurred around 500 °C indicating the decomposition of octyl moieties.[13] For E-OMSN and K-OMSN large weight loss values of 19.6 % and 32.5 % were recorded, respectively. Also, two sharp decreases were observed in spectra of peptide coated particles around 400 °C and 500 °C, which correspond to decomposition of PAs and octyl groups, respectively. For bare peptide amphiphiles, almost all weight was lost at 800 °C. Based on the TGA results, we calculated grafting densities of the PA molecules onto the OMSN surfaces (see ESI† for details).[40-41] The grating densities of E-OMSNs and K-OMSNs were 0.94 and 2.95 PA/nm^2, respectively, indicating the surface of OMSNs were densely covered by the peptide molecules. The higher grafting density for K-OMSN was observed due to the electrostatic interactions between positively charged K-PA and unreacted surface silanol groups of OMSNs. Average particles sizes of the MSNs and OMSNs were calculated to be 100 nm and 104 nm, respectively from the TEM images (Table 1). The 4 nm increase in the particle size after octyl addition shows the ~2 nm shell formation around the particles. Hydrodynamic sizes of the MSN, E-MSN and K-MSN were measured by using dynamic light scattering technique (Table 1 and ESI†, Fig. S5).

Table 1. Physical properties of bare, octyl modified and peptide functionalized MSNs.

Sample	TEM Size (nm)	DLS Size (nm)	Zeta potential (mV)
MSN	99.8 ± 20.7	166.5 ± 8.0	-36.6 ± 1.1
OMSN	104.3 ± 21.5	N/A	N/A
E-OMSN	N/A	143.8 ± 19.8	-38.0 ± 0.8
K-OMSN	N/A	145.2 ± 1.6	-25.1 ± 0.7

The OMSN is water insoluble and it is not possible to measure its hydrodynamic size. Hydrodynamic sizes of the peptide coated particles are slightly larger (around 40 nm) than their primary particle sizes (size of OMSN) due to the slight aggregation in aqueous media for these particles. On the other hand, aggregation becomes more pronounced for bare MSNs with a 67 nm difference between hydrodynamic and primary particle sizes. This difference could be explained by the fact that two different techniques, TEM and DLS, were used for the measurements. While dried samples were used for TEM imaging, hydrodynamic size of particles was measured with DLS where interactions with solvent molecules are also taken into account. The surfaces of the particles were characterized by measuring their zeta potentials (Table 1). Bare MSN surface is negatively charged (-37 mV) due

to the surface silanol groups.[10] Modifying MSN surface with a negatively charged E-PA did not significantly affect the zeta potential of the surface (-38 mV) since both silanol and E-PA groups are negatively charged. Coating MSN surface with positively charged K-PA, on the other hand, resulted in a remarkable increase in the zeta potential (-25 mV).

Cyto-compatibility of MSNs

Good compatibility of therapeutic nanoparticles with biological organism is necessary to prevent possible side effects of these therapies. Accordingly, *in vitro* cytocompatibility of the peptide coated and bare MSNs were evaluated by using HUVEC and A10 cell lines. The viability of the cells treated with different particle concentrations (10 to 200 μg mL^{-1}) was studied by using Alamar

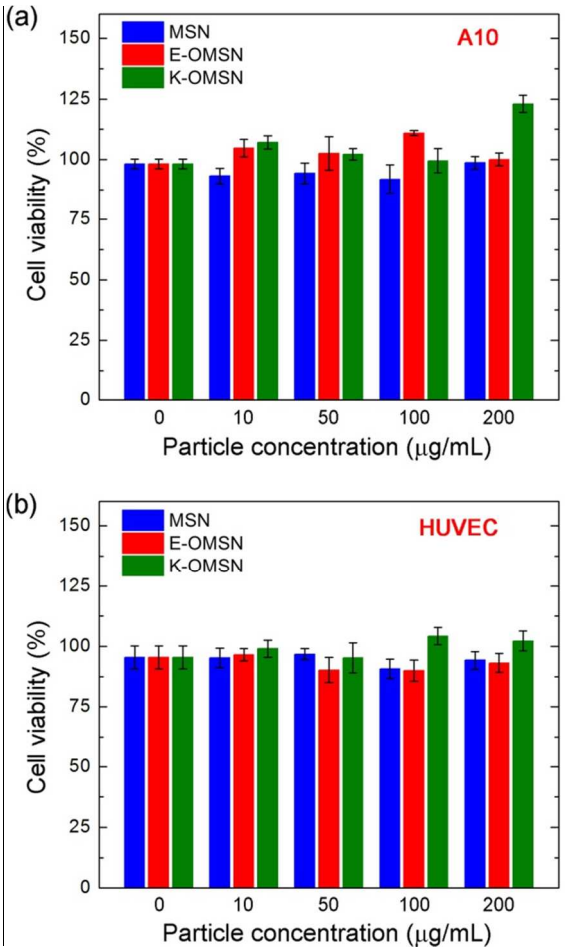

Fig. 4 Cytotoxicity results of bare and peptide functionalized MSNs. (a) A10 cells incubated for 4 h with particles and 20 h in particle free media, (b) HUVEC cells incubated for 4 h with particles and 20 h in particle free media.

blue assay. First, cells were treated with particles for 4 h and then incubated for additional 20 h in particle free media. None of the particles showed decrease in viability of both cell lines even at very high particle concentration of 200 μg mL^{-1} (Fig. 4a, b).

Cellular uptake studies

Improving cellular uptake of the therapeutic nanoparticles is essential for enhancing their efficacy. Therefore, we studied the uptake of the particles by A10 and HUVEC cells by using confocal microscopy and flow cytometer techniques. Both A10 and HUVEC cells were treated with 200 μg mL^{-1} nanoparticles for 4 h and the cells were analyzed after 20 h of further incubation. As shown in Fig. 5, confocal microscopy revealed that the peptide coated particles were internalized remarkably more than the bare MSNs by both cell lines.

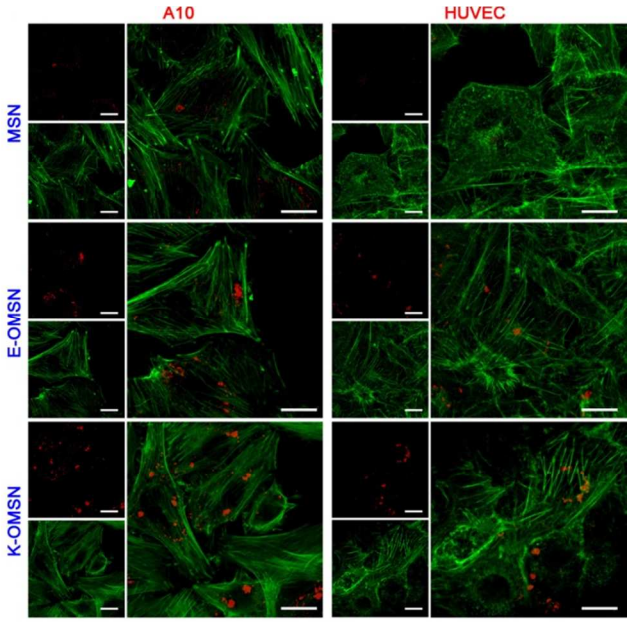

Fig. 5 Uptake results of bare and peptide functionalized MSNs. Confocal results showing that peptide functionalized particles internalized more in both A10 and HUVEC cell lines. Upper images at left shows the fluorescence of particles, lower images at left shows the fluorescence of actin filaments stained by Phalloidin-TRITC and panels at right shows the merge images.

In order to compare the uptake amount of the particles, fluorescence of the internalized particles was quantified by using flow cytometer.

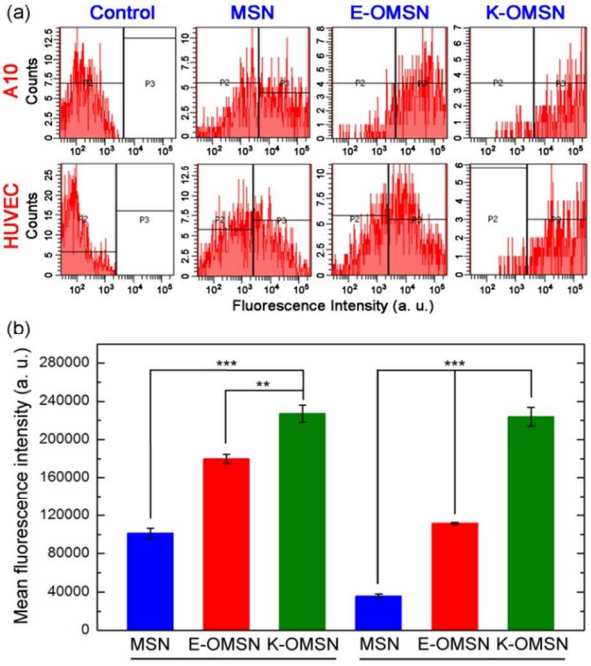

Fig. 6 Flow cytometry analysis of A10 and HUVECs treated with bare and peptide functionalized MSNs. (a) Flow cytometry histograms. (b) Graph demonstrated the improved uptake of peptide functionalized MSNs. Data were generated from at least three independent experiments. According to Student's t test, **p < 0.001 and ***p < 0.0001

More uptake was observed for K-OMSN in both cell lines. The amount of internalized fluorescent E-OMSNs was less than K-OMSNs, however, they were internalized more than bare particles. The uptake of K-OMSN by A10 and HUVEC cells was 2.3 and 6.3 fold larger than the uptake of MSN, respectively. Also, E-OMSN demonstrated 1.8 and 3.1 fold increased uptake by A10 and HUVEC cells, respectively, compared to bare MSNs. It is well known that positively charged surfaces can electrostatically interact with the slightly negatively charged cell membrane.[42] Therefore, highest cellular internalization was observed for positively charged K-PA functionalized K-OMSN. Although, both MSN and E-OMSN samples have about the same zeta potential values, around -40 mV, cellular uptake of E-OMSNs was significantly higher than the MSNs. This observation indicates that uptake rate and amount of the nanoparticles cannot be simply correlated with net surface charge of the surface; instead, it is more related with the chemical structure of the surface functional groups.

Conclusions

In summary, we developed a straightforward method to functionalize MSNs with short peptide chains by using self-assembly of PAs around the hydrophobic MSNs. The resulting peptide functionalized particles can be easily dispersed in the aqueous media. We observed that peptide functionalized MSNs are not toxic to the A10 and HUVEC cell lines up to a high dose of 100 μg mL^{-1}. In addition, it was observed that cellular uptake of MSNs can be enhanced up to 6.3 fold by coating them with PAs, especially positively charged ones. We believe that the facile method demonstrated in this study can be applied to prepare MSNs with diverse functionalities including cancer cell targeting, cell penetrating properties and responsive drug release, by simply changing the peptide signal to achieve selective bioactive properties.

Acknowledgements

M.S., D.M. and A.Y. are supported by TUBITAK-BIDEB PhD fellowships. FACS analyses were performed at Diskapi Yildirim Beyazit Training and Research Hospital, and we thank E. Calisir, Prof. T. Delibasi and ADAcell for help in FACS experiments. M.O.G and A.B.T. acknowledge support from the Turkish Academy of Sciences Distinguished Young Scientist Award (TUBA-GEBIP).

Notes and references

[a]*National Nanotechnology Research Center (UNAM), Bilkent University, 06800 Ankara, Turkey.*
[b]*Institute of Materials Science and Nanotechnology, Bilkent University, 06800 Ankara, Turkey*
† E-mail: moguler@unam.bilkent.edu.tr, ademy@bilkent.edu.tr, atekinay@unam.bilkent.edu.tr
Fax: +90 312 266 4365; Tel: +90 312 290 3552
Electronic supplementary information (ESI) available
‡These authors contributed equally.

See DOI: 10.1039/b000000x/

1. K. T. Mody, A. Popat, D. Mahony, A. S. Cavallaro, C. Yu and N. Mitter, *Nanoscale*, 2013, **5**, 5167-5179.
2. J. E. Lee, N. Lee, T. Kim, J. Kim and T. Hyeon, *Accounts. Chem. Res.*, 2011, **44**, 893-902.
3. S.-H. Wu, Y. Hung and C.-Y. Mou, *Chem. Commun.* , 2011, **47**, 9972-9985.
4. J. Lu, M. Liong, J. I. Zink and F. Tamanoi, *Small*, 2007, **3**, 1341-1346.
5. C. Liu, J. Guo, W. Yang, J. Hu, C. Wang and S. Fu, *J. Mater. Chem.*, 2009, **19**, 4764-4770.
6. Y.-S. Lin, C.-P. Tsai, H.-Y. Huang, C.-T. Kuo, Y. Hung, D.-M. Huang, Y.-C. Chen and C.-Y. Mou, *Chem. Mater.*, 2005, **17**, 4570-4573.
7. S. Sharifi, S. Behzadi, S. Laurent, M. L. Forrest, P. Stroeve and M. Mahmoudi, *Chem. Soc. Rev.* , 2012, **41**, 2323-2343.
8. S. P. Hudson, R. F. Padera, R. Langer and D. S. Kohane, *Biomaterials*, 2008, **29**, 4045-4055.
9. Y. Zhao, X. Sun, G. Zhang, B. G. Trewyn, I. I. Slowing and V. S.-Y. Lin, *ACS Nano*, 2011, **5**, 1366-1375.
10. A. Yildirim, E. Ozgur and M. Bayindir, *J. Mater. Chem. B*, 2013, **1**, 1909-1920.
11. L.-S. Wang, L.-C. Wu, S.-Y. Lu, L.-L. Chang, I.-T. Teng, C.-M. Yang and J.-a. A. Ho, *ACS Nano*, 2010, **4**, 4371-4379.
12. Q. He, J. Zhang, J. Shi, Z. Zhu, L. Zhang, W. Bu, L. Guo and Y. Chen, *Biomaterials*, 2010, **31**, 1085-1092.
13. A. Yildirim, G. B. Demirel, R. Erdem, B. Senturk, T. Tekinay and M. Bayindir, *Chem. Commun.*, 2013, **49**, 9782-9784.
14. J. T. Sun, Z. Q. Yu, C. Y. Hong and C. Y. Pan, *Macromol. Rapid Comm.* , 2012, **33**, 811-818.
15. M. Ma, H. Chen, Y. Chen, K. Zhang, X. Wang, X. Cui and J. Shi, *J. Mater. Chem.*, 2012, **22**, 5615-5621.
16. M. Liong, J. Lu, M. Kovochich, T. Xia, S. G. Ruehm, A. E. Nel, F. Tamanoi and J. I. Zink, *ACS nano*, 2008, **2**, 889-896.
17. N. Erathodiyil and J. Y. Ying, *Accounts. Chem. Res.*, 2011, **44**, 925-935.
18. M. M. van Schooneveld, E. Vucic, R. Koole, Y. Zhou, J. Stocks, D. P. Cormode, C. Y. Tang, R. E. Gordon, K. Nicolay and A. Meijerink, *Nano letters*, 2008, **8**, 2517-2525.
19. C. E. Ashley, E. C. Carnes, G. K. Phillips, D. Padilla, P. N. Durfee, P. A. Brown, T. N. Hanna, J. Liu, B. Phillips and M. B. Carter, *Nat. Mater.*, 2011, **10**, 389-397.
20. S. Sulek, B. Mammadov, D. I. Mahcicek, H. Sozeri, E. Atalar, A. B. Tekinay and M. O. Guler, *J. Mater. Chem.*, 2011, **21**, 15157-15162.
21. R. M. Levine, C. M. Scott and E. Kokkoli, *Soft Matter*, 2013, **9**, 985-1004.
22. D. P. Ferris, J. Lu, C. Gothard, R. Yanes, C. R. Thomas, J. C. Olsen, J. F. Stoddart, F. Tamanoi and J. I. Zink, *Small*, 2011, **7**, 1816-1826.
23. K. Epler, D. Padilla, G. Phillips, P. Crowder, R. Castillo, D. Wilkinson, B. Wilkinson, C. Burgard, R. Kalinich and J. Townson, *Adv. Healthcare Mater.*, 2012, **1**, 348-353.

24. S.-H. Cheng, C.-H. Lee, M.-C. Chen, J. S. Souris, F.-G. Tseng, C.-S. Yang, C.-Y. Mou, C.-T. Chen and L.-W. Lo, *J. Mater. Chem.* , 2010, **20**, 6149-6157.
25. Y. Wang, W. Shi, W. Song, L. Wang, X. Liu, J. Chen and R. Huang, *J. Mater. Chem.*, 2012, **22**, 14608-14616.
26. L. Pan, Q. He, J. Liu, Y. Chen, M. Ma, L. Zhang and J. Shi, *J. Am. Chem. Soc.*, 2012, **134**, 5722-5725.
27. X. Li, Y. Chen, M. Wang, Y. Ma, W. Xia and H. Gu, *Biomaterials*, 2013, **34**, 1391-1401.
28. I. L. Medintz, T. Pons, J. B. Delehanty, K. Susumu, F. M. Brunel, P. E. Dawson and H. Mattoussi, *Bioconjugate Chem.* , 2008, **19**, 1785-1795.
29. S.-f. Ye, M.-m. Tian, T.-x. Wang, L. Ren, D. Wang, L.-h. Shen and T. Shang, *Nanomed-Nanotechnol.*, 2012, **8**, 833-841.
30. C. Coll, L. Mondragón, R. Martínez-Máñez, F. Sancenón, M. D. Marcos, J. Soto, P. Amorós and E. Pérez-Payá, *Angew. Chem. Int. Edit.*, 2011, **50**, 2138-2140.
31. G.-F. Luo, W.-H. Chen, Y. Liu, J. Zhang, S.-X. Cheng, R.-X. Zhuo and X.-Z. Zhang, *J. Mater. Chem. B*, 2013, **1**, 5723-5732.
32. M. Oishi, A. Tamura, T. Nakamura and Y. Nagasaki, *Adv. Funct. Mater.*, 2009, **19**, 827-834.
33. Y. Choi, Y. Cho, M. Kim, R. Grailhe and R. Song, *Anal. Chem.*, 2012, **84**, 8595-8601.
34. D. Deng, D. Zhang, Y. Li, S. Achilefu and Y. Gu, *Biosens. Bioelectron.*, 2013, **49**, 216-221.
35. I. M. Rio-Echevarria, R. Tavano, V. Causin, E. Papini, F. Mancin and A. Moretto, *J. Am. Chem. Soc.*, 2010, **133**, 8-11.
36. B. Baudin, A. Bruneel, N. Bosselut and M. Vaubourdolle, *Nature protocols*, 2007, **2**, 481-485.
37. A. Yildirim, H. Budunoglu, B. Daglar, H. Deniz and M. Bayindir, *ACS Appl. Mater. Interfaces* 2011, **3**, 1804-1808.
38. V. Cauda, A. Schlossbauer, J. Kecht, A. Zu□rner and T. Bein, *J. Am. Chem. Soc.* , 2009, **131**, 11361-11370.
39. L. Zhuravlev, *Langmuir*, 1987, **3**, 316-318.
40. M. Kar, P. Vijayakumar, B. Prasad and S. S. Gupta, *Langmuir*, 2010, **26**, 5772-5781.
41. D. Kim, S. Finkenstaedt-Quinn, K. R. Hurley, J. T. Buchman and C. L. Haynes, *Analyst*, 2014, DOI: 10.1039/c3an01679j
42. L. Chen, J. M. Mccrate, J. C. Lee and H. Li, *Nanotechnology*, 2011, **22**, 105708.